Journal of Alloys and Compounds 480 (2009) 104–106

Contents lists available at ScienceDirect

Journal of Alloys and Compounds

journal homepage: www.elsevier.com/locate/jallcom

Anisotropic optical characteristics of Au-doped rhenium diselenide single crystals

D.O. Dumcenco[a], W.Y. Huang[a], Y.S. Huang[a,*], K.K. Tiong[b]

[a] Department of Electronic Engineering, National Taiwan University of Science and Technology, Taipei 106, Taiwan, ROC
[b] Department of Electrical Engineering, National Taiwan Ocean University, Keelung 202, Taiwan, ROC

ARTICLE INFO

Article history:
Received 19 June 2008
Received in revised form 9 September 2008
Accepted 25 September 2008
Available online 20 November 2008

PACS:
78.20.−e
78.40.Fy
78.55.Hx

Keywords:
Transition-metal dichalcogenides
Polarized piezoreflectance
Photoreflectance
Excitons

ABSTRACT

We report the anisotropic optical property study on the band-edge excitonic transitions of $ReSe_2$ single crystals doped with Au. The temperature-dependent piezoreflectance (PzR) and photoreflectance (PR) spectra with $\mathbf{E}||\mathbf{b}$ and $\mathbf{E}\perp\mathbf{b}$ polarizations in the near band-edge region provide conclusive evidence that band-edge excitonic transition features, namely E_1^{ex}, and E_2^{ex}/E_3^{ex} are from different origins. The features located at higher energy side correspond to the Rydberg series starting with principal quantum number $n = 2$. The doping effects were presented and discussed.

1. Introduction

Rhenium diselenide ($ReSe_2$) is a diamagnetic semiconductor belonging to the family of transition-metal dichalcogenides crystallized in a distorted $CdCl_2$ structure of triclinic symmetry with clustering of Re_4 diamond units forming a one-dimensional chain along the **b**-axis within the van der Waals plane [1,2]. Crystals with triclinic symmetry are optically biaxial with in-plane anisotropy along and perpendicular to the **b**-axis. $ReSe_2$ is a subject of considerable interest because of its anisotropic properties and potential application as a promising solar-cell material for efficient photoelectrochemical cells [3,4].

In this paper, we report the polarization-dependent optical properties study of Au-doped $ReSe_2$ single crystals. The temperature-dependent piezoreflectance (PzR) and photoreflectance (PR) measurements with $\mathbf{E}||\mathbf{b}$ and $\mathbf{E}\perp\mathbf{b}$ polarizations were carried out in the region of 1.35–1.52 eV. The transition energies and broadening parameters of the observed polarization-dependent excitonic features for Au-doped were determined and compared with the undoped one to study the doping effects of Au on the optical properties of $ReSe_2$.

2. Experimental details

The $ReSe_2$ single crystals doped with Au (denoted as $ReSe_2$:Au) were grown by the chemical vapor transport method with bromine as a transport agent [5]. The weight of doping material was determined stoichiometrically to obtain the small concentration of dopant, i.e. 50 mg of Au on about 10 g of the total charge weight. $ReSe_2$:Au single crystals formed thin silver-colored, graphite-like platelets up to 50 mm^2 (10 mm × 5 mm) in area and ~100 μm in thickness. X-ray diffraction patterns confirmed the triclinic symmetry of the single crystals with all parameters consistent with those previously reported [2]. Auger electron spectroscopy (AES) [6] was utilized to examine the Au content of the crystals. The results showed an average ~0.15 at.% concentration of Au in the sample crystals. Considerable discrepancy exists between the nominal doping ratio and that determined by AES, indicating that Re and Au were chemically transported at different rate and most of the Au must remain in the untransported residual charge. It is also noted that the Au-doped single crystals become easy to separate along **b**-axis in comparison with the undoped ones.

The PzR/PR apparatus has been described in Ref. [7]. The PzR measurement was achieved by gluing the thin single crystal specimens on a 0.15 cm thick lead–zirconate–titanate piezoelectric transducer driven by a 200 V_{rms} sinusoidal wave at 200 Hz. The CASIX Rochon prisms were employed for polarization-dependent measurements. PR measurement was achieved using an internally modulated 670 nm laser diode served as the pumping beam. The temperature-dependent measurements were made between 15 and 300 K with the temperature stability of 0.5 K or better.

---

[*] Corresponding author. Tel.: +886 2 27376385; fax: +886 2 27376424.
E-mail address: ysh@mail.ntust.edu.tw (Y.S. Huang).

0925-8388/$ – see front matter © 2008 Elsevier B.V. All rights reserved.
doi:10.1016/j.jallcom.2008.09.174

3. Results and discussion

Fig. 1 depicts the polarization dependence of PzR and PR spectra for $ReSe_2$:Au in the energy range of 1.35–1.52 eV at 15 K. As seen in Fig. 1, in the vicinity of direct band edge, feature 1 (denoted as E_1^{ex}) is present in the **E**||**b** polarization while features 2 and 3, denoted as E_2^{ex} and E_3^{ex}, only appear in the **E**⊥**b** polarization. This provides conclusive evidence that feature 1 and features 2 and 3 are associated with the excitonic transitions from different origins. This observation is different from the isostructural compound ReS_2 where only E_1^{ex} and E_2^{ex} features were detected [8].

The PzR and PR spectra have been fitted by a Lorentzian lineshape expression [9],

$$\frac{\Delta R}{R} = Re\left[\sum_{i=1}^{n} A_i^{ex} e^{j\varphi_i^{ex}} (E - E_i^{ex} + j\Gamma_i^{ex})^{-2}\right], \qquad (1)$$

where A_i^{ex} and φ_i^{ex} are, respectively, the amplitude and phase of the lineshape, and E_i^{ex} and Γ_i^{ex} are, respectively, the transition energy and broadening parameter of the excitonic transitions. The values of energy and broadening parameters of excitonic transitions determined are $E_1^{ex} = 1.386 \pm 0.002$ eV, $E_2^{ex} = 1.410 \pm 0.002$ eV, $E_3^{ex} = 1.449 \pm 0.002$ eV and $\Gamma_1^{ex} = 4.9 \pm 1.0$ meV, $\Gamma_2^{ex} = 6.0 \pm 1.0$ meV, $\Gamma_3^{ex} = 6.5 \pm 1.0$ meV, respectively. In comparison with previous study of undoped $ReSe_2$ [10], the presented results show that the band-edge excitonic transition energies are not sensitive to a small concentration of Au doping, and broadening parameters are slightly increased due to impurity scattering. These observations agree with the results reported previously for Nb-doped ReS_2 single crystals [8].

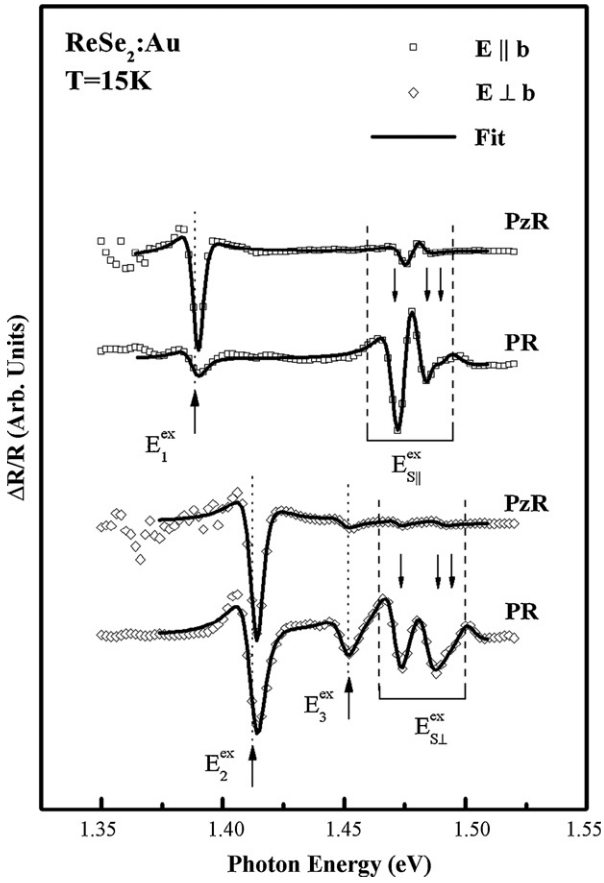

Fig. 1. Polarized PzR and PR spectra of $ReSe_2$:Au at 15 K. The open-squares and open-diamonds curves correspond, respectively, to **E**||**b** and **E**⊥**b** polarizations. The solid curves are the least squares fits to Eq. (1).

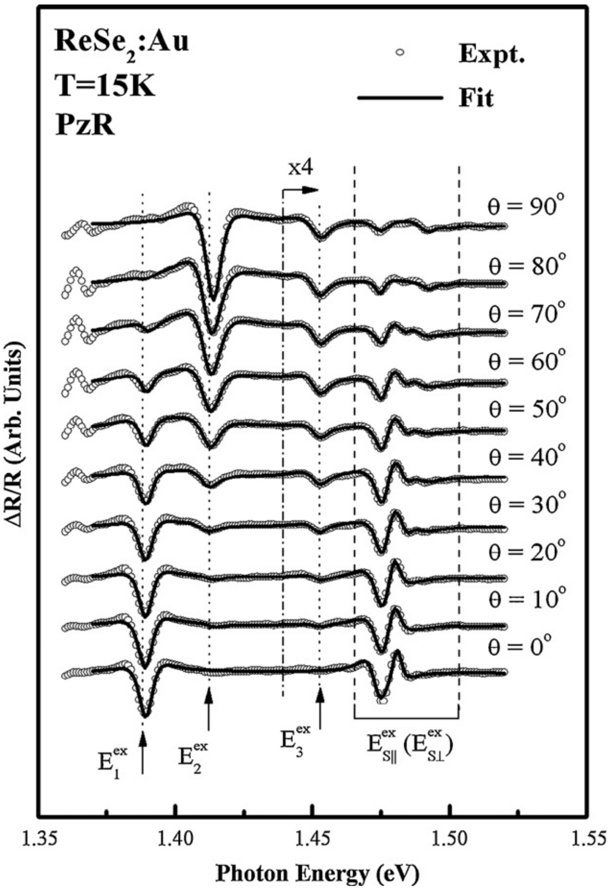

Fig. 2. Polarized PzR spectra of $ReSe_2$:Au (open-circles curves) with polarization angle ranging from $\theta = 0^\circ$ (**E**||**b**) to $\theta = 90^\circ$ (**E**⊥**b**). The solid curves are the least squares-fits to Eq. (1).

As shown in Fig. 1, each of the polarized PR spectra shows prominent and enlarged features of the excitonic series $E_{S||}^{ex}$ or $E_{S\perp}^{ex}$, positioned at the higher energy side with respect to the band-edge excitons. Photo-induced modification of the reflectivity has been proposed to account for the enhancements of excitonic series in the low-temperature PR spectra [7]. The analysis of higher energy side sequences $E_{S||(S\perp)}^{ex}$ reveals that excitonic features can be further analyzed by using the Rydberg series starting with principal quantum number $n = 2$ [11]. Through accurate fitting with the Rydberg sequence formula, the transition energies in the excitonic sequence are matched well with the energy positions of exciton levels $n = 2$, 3, 4. These excitonic transitions are similar to the so-called yellow exciton series 2p, 3p, 4p as observed in Cu_2O [11]. The values of the threshold energy $E_{S||}^{n=\infty} = 1.495 \pm 0.004$ eV ($E_{S\perp}^{n=\infty} = 1.502 \pm 0.004$ eV) and the effective Rydberg constant $R_{S||}^* = 101 \pm 7$ meV ($R_\perp^* = 128 \pm 7$ meV) corresponds to the 1s orbital binding energy ($n = 1$), are respectively obtained from the fits. The crystal anisotropy along and perpendicular to **b**-axis results in the splitting of the valance band and hence in the difference of threshold energies, determined to be $\Delta E \approx E_{S\perp}^{n=\infty} - E_{S||}^{n=\infty} \approx 7$ meV. The results are in good agreement with those previously obtained for ReS_2 [7].

The polarized nature of band-edge excitons E_1^{ex}, E_2^{ex} and E_3^{ex} in $ReSe_2$:Au were further characterized using angular dependent PzR measurements at 15 K. The polarized PzR spectra with polarization angles ranging from $\theta = 0^\circ$ (**E**||**b**) to $\theta = 90^\circ$ (**E**⊥**b**) are shown in Fig. 2. The signal intensity of E_1^{ex} decreased, while the amplitudes of E_2^{ex} and E_3^{ex} enlarged when the angle θ of linearly polarized light increased from 0° to 90°. The angular dependence of the amplitudes

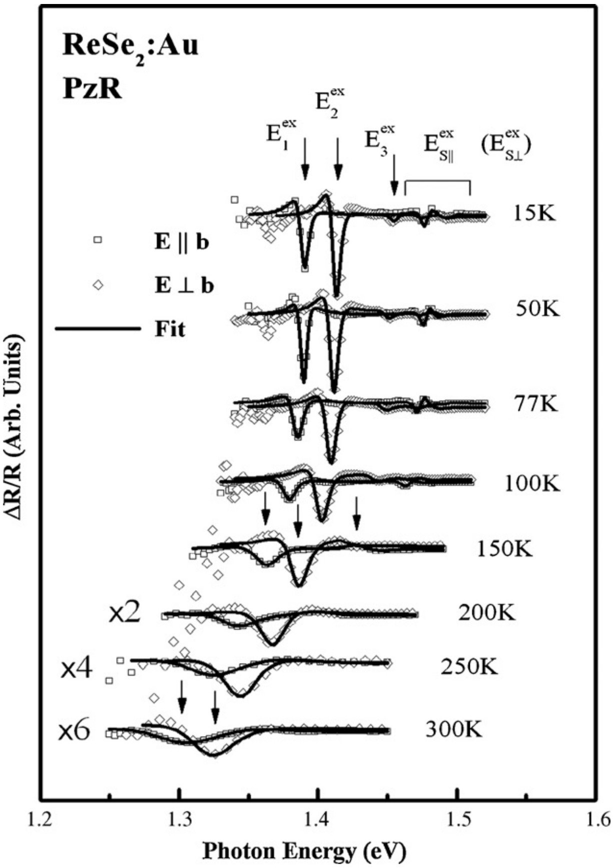

Fig. 3. Temperature-dependent polarized PzR spectra of $ReSe_2$:Au at several temperatures between 15 and 300 K. The open-squares and open-diamonds curves correspond to the experimental data of **E**||**b** and **E**⊥**b** polarizations, respectively, and the solid curves are least squares-fits to Eq. (1).

obtained shows a sinusoidal variation with respect to the angular change of the linearly polarized light that corresponds to Malus' law [12]. The polarization sensitive behavior of E_1^{ex} and E_2^{ex}/E_3^{ex} provides potential usage for $ReSe_2$ to fabricate a polarization sensitive photodetector applied in multi-channel optical communications for detecting the various orientations of linearly polarized light [13].

Temperature-dependent PzR spectra of $ReSe_2$:Au with the **E**||**b** and **E**⊥**b** polarizations are shown in Fig. 3. The results in Fig. 3 show that up to 175 K the higher order features of the excitonic sequence are ionized. At a still higher temperature, full ionization process renders the interband excitonic sequence undetectable. The temperature-dependent transition energies of band-edge excitons E_1^{ex}, E_2^{ex} and E_3^{ex} were fitted by Varshni semiempirical relationship [14]: $E(T) = E(0) - \alpha T^2/(\beta + T)$. Where α is related to the electron–phonon interaction and β is closely related to the Debye temperature. Varshni coefficients α and β are determined to be 0.53 ± 0.05 meV/K and 210 ± 75 K, 0.54 ± 0.05 meV/K and 210 ± 75 K, and 0.51 ± 0.05 meV/K and 210 ± 75 K for E_1^{ex}, E_2^{ex} and E_3^{ex}, respectively. The results are quite similar to the values of previous reports on undoped $ReSe_2$ [10].

The temperature dependence of the linewidth was fitted by $\Gamma(T) = \Gamma_0 + \Gamma_{LO}/[\exp(\Theta_{LO}/T) - 1]$ [15]: the first term Γ_0, represents broadening invoked from temperature-independent mechanisms, while the second term is caused by the Fröhlich interaction described by the strength of the electron (exciton)–LO phonon coupling Γ_{LO} and LO phonon temperature Θ_{LO} parameters. The values of the coupling constant Γ_{LO} determined to be 65 ± 15 meV, 50 ± 15 meV and 71 ± 20 meV for E_1^{ex}, E_2^{ex} and E_3^{ex}, respectively, are considerably larger than those reported for a number of semiconductors. We suspected that the large values of Γ_{LO} may be the general characteristics of crystals with layer structure.

4. Summary

The anisotropic optical properties of $ReSe_2$:Au single crystals were studied by polarized PzR and PR measurements. In addition to higher energy excitonic series, three band-edge excitonic features are observed. The E_1^{ex} feature is present in the **E**||**b** polarization while E_2^{ex} and E_3^{ex} features appeared in the **E**⊥**b** polarization. The higher energy excitonic series are similar to the so-called yellow exciton series as observed in Cu_2O, which starts from the excitonic level $n = 2$. The values of band-edge excitonic transition energies E_1^{ex}, E_2^{ex} and E_3^{ex} of $ReSe_2$:Au remain practically unchanged in comparison with undoped $ReSe_2$. Nevertheless, the Au-doping effect shows up in a slight increase of the broadening parameter of the excitonic features.

Acknowledgement

The authors acknowledge the supports of National Science Council of Taiwan under Project No. NSC 96-2221-E-011-030.

References

[1] J.A. Wilson, A.D. Yoffe, Adv. Phys. 18 (1969) 193–335.
[2] J.C. Wildervanck, F. Jellinek, J. Less-Common Metals 24 (1971) 73–81.
[3] B.L. Wheeler, J.K. Leland, A.J. Bard, J. Electrochem. Soc. 133 (1986) 358–361.
[4] B. Schubert, H. Tributsch, J. Appl. Electrochem. 20 (1990) 786–792.
[5] Y.S. Huang, C.H. Ho, P.C. Liao, K.K. Tiong, J. Alloys Compd. 262/263 (1997) 92–96.
[6] D.K. Schroder, Semiconductor Material and Device Characterization, 2nd ed., Wiley, New York, 1998, p. 671.
[7] C.H. Ho, P.C. Yen, Y.S. Huang, K.K. Tiong, Phys. Rev. B 66 (1–5) (2002) 245207.
[8] D.O. Dumcenco, Y.S. Huang, C.H. Liang, K.K. Tiong, J. Appl. Phys. 102 (1–7) (2007) 083523.
[9] D.E. Aspnes, in: M. Balkanski (Ed.), Handbook on Semiconductors, vol. 2, North-Holland, Amsterdam, 1980, pp. 109–154.
[10] C.H. Ho, P.C. Liao, Y.S. Huang, K.K. Tiong, Phys. Rev. B 55 (1997) 15608–15613.
[11] P.Y. Yu, M. Cardona, Fundamentals of Semiconductors, 3rd ed., Springer, New York, 2001.
[12] G.A. Medvedkin, Yu.V. Rud, M.A. Tairov, Phys. Stat. Sol. (a) 115 (1989) 11–50.
[13] C.H. Ho, H.W. Lee, C.C. Wu, J. Phys.: Condens. Matter 16 (2004) 5937–5944.
[14] Y.P. Varshni, Physica 34 (1967) 149–153.
[15] P. Lautenschlager, M. Garriga, L. Vina, M. Cardona, Phys. Rev. B 36 (1987) 4821–4830.